UV-Photolysis of HI···CO_2 Complexes in Solid Parahydrogen: Formation of CO and H_2O†

Mizuho Fushitani,‡ Tadamasa Shida,‡,§ Takamasa Momose,*,‡ and Markku Räsänen*,||

Division of Chemistry, Graduate School of Science, Kyoto University, Kyoto 606-8502, Japan, Department of Chemistry, Kanagawa University, Hiratsuka, Kanagawa 259-1293, Japan, and Laboratory of Physical Chemistry, P.O. Box 55 (A. I. Virtasen Aukio 1), FIN-00014, University of Helsinki, Finland

Received: October 29, 1999; In Final Form: January 10, 2000

The photochemistry of $(HI)_m$···$(CO_2)_n$ (m, n = 1, 2, ...) complexes trapped in solid parahydrogen was studied by Fourier transform infrared absorption spectroscopy. Photolysis of the HI in the HI···$(CO_2)_n$ complexes results in the generation of carbon monoxide and water molecules along with iodine atoms. Analysis of the observed spectra leads to the conclusion that the energetic hydrogen atom produced by the photolysis of HI initiates the reaction with one of the CO_2 molecules in the complexes as H + CO_2 → OH + CO, which is followed by the secondary reaction of OH radicals with the matrix hydrogen as OH + H_2 → H_2O + H. These four-atom reactions are of practical importance in combustion processes as well as of theoretical importance in fundamental chemical dynamics. The result of the present study shows the usefulness of the parahydrogen matrix for fundamental study of photochemistry with the use of weakly bound complexes.

1. Introduction

Photolysis of trapped molecules in a low-temperature solid provides convenient means for spectroscopic studies of photoproducts and intermediates. As for single molecules isolated in the solid, photoexcitation may induce dissociation or isomerization of the molecules. If the cage barrier of the solid is low enough compared with excess kinetic energies of photofragments, they may be permanently separated. If, on the other hand, the fragments do not have enough kinetic energies to escape from the cage, recombination may produce new species in the cage. The cage-exit energies required for the permanent separation of the photofragments are on the order of ∼0.5−1.5 eV for hydrogen atoms and higher for heavier particles in the familiar rare gas matrixes. Thus, isomerization and cage recombination are predominant for the most photofragments.[1]

Meanwhile, solid parahydrogen (p-H_2) is found to be a superior matrix for both high-resolution vibration−rotation spectroscopy[2,3] and the study of photochemical processes.[4−6] This feature is due to the extremely weak intermolecular interaction in solid hydrogen. The cage-exit barrier in solid hydrogen is very low compared with the rare gas matrixes, which allows us to study photodissociation of trapped molecules with ease. Furthermore, being a molecular matrix, a hydrogen molecule in the solid may participate in secondary chemical reactions with reactive radicals produced *in situ* photolysis of precursors.[6,7] In such reactions at cryogenic temperatures quantum tunneling may be important,[7] which is interesting in its own right.

Weakly bound complexes with a fixed structure in solid p-H_2 are even more interesting than single molecules because such complexes may be regarded as a prearranged reactant system in photoinduced bimolecular reactions. The weak intermolecular interaction and the large cage dimension of solid p-H_2 allow the accommodation of sizable complexes with little perturbation. In this paper, we report a spectroscopic study of photochemistry of $(HI)_m$···$(CO_2)_n$ (m, n = 1, 2, ...) complexes trapped in solid p-H_2. Low-pressure mercury lamp irradiation results in the disappearance of the infrared absorption of HI and the appearance of the spin−orbit absorption of iodine atoms.[8,9] In addition, the absorptions of CO and H_2O are also observed to our surprise. The findings are successfully accounted for.

2. Experiments

Hydrogen iodide (HI) was synthesized by the reaction of iodine and tetralin at 207 °C.[10] The produced HI vapor was purified by passing through a tetralin trap before condensing in a trap at liquid nitrogen temperature. The gas was further purified by low-temperature distillation in a vacuum line.

The preparation of crystalline p-H_2 samples was performed in the same way as reported previously.[3,11] Almost pure p-H_2 gas (with the residual orthohydrogen less than 0.01%) was obtained by passing normal hydrogen gas through a hydrous ferric oxide catalyst at 13.8 K. The p-H_2 gas thus converted was mixed with the vapor of CO_2 and HI. The mixing ratio of CO_2/HI/p-H_2 was $1:16:5\times10^5$ and $15:1:2\times10^6$. The mixed gas was then introduced slowly into an optical cell which was kept at 8.0 K during the crystallization.

All the infrared measurement and irradiation were carried out at 4.9 K. Fourier transform infrared (FTIR) spectra were recorded by a Bruker IFS 120 HR spectrometer with a resolution of 0.1 and 0.01 cm^{-1}. A globar and a tungsten lamp were used as the light source with a KBr beam splitter and a liquid N_2 cooled InSb and MCT detector. A 20 W low-pressure mercury lamp which mainly emits light at 253.7 nm with a small fraction of light at 184.9 nm was used without filters for the photolysis.

3. Results

3.1. System of CO_2/HI/p-H_2 = 1:16:5×10^5. FTIR spectra of the sample with a composition of CO_2/HI/p-H_2 = $1:16:5\times10^5$

† Part of the special issue "Marilyn Jacox Festschrift".

* To whom correspondence should be addressed. E-mail: momose@kuchen.kyoto-u.ac.jp; morasane@pcu.helsinki.fi.

‡ Kyoto University.

§ Kanagawa University.

|| University of Helsinki.

10.1021/jp9938462 CCC: $19.00 © 2000 American Chemical Society
Published on Web 03/15/2000

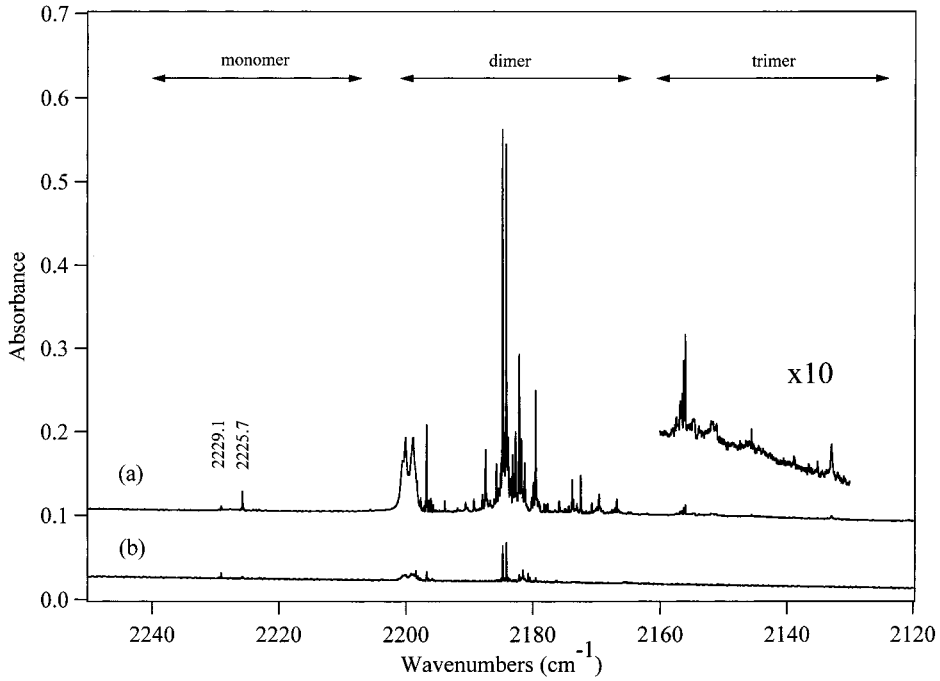

Figure 1. FTIR spectra in the HI stretching region of a sample in solid parahydrogen with a composition of CO_2/HI/*p*-H_2 = 1:16:5×10^5: (a) the sample immediately after the deposition; (b) same as (a) after a continual 1020 min UV irradiation. The horizontal arrows indicate the spectral region is divided into three groups of HI, $(HI)_2$, and $(HI)_3$ clusters which are little affected by CO_2.

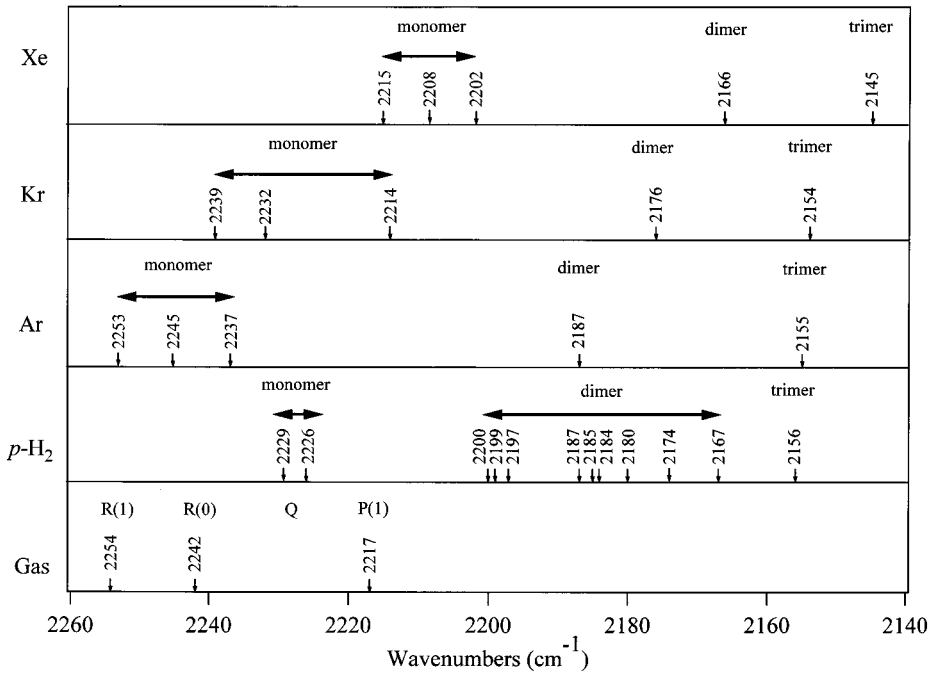

Figure 2. Collection of the spectral information on the HI stretching vibration for monomer, dimers, and trimers. The references for Xe, Kr, and Ar matrixes are refs 12, 13, and 14, respectively. The stick spectrum for *p*-H_2 is constructed by reproducing the major observed peaks in Figure 1a. The frequencies of gaseous HI were measured at room temperatures with the spectrometer described in the Experimental Section.

in the HI absorption region are shown in Figure 1. The composition was chosen to have HI dominantly over CO_2. Traces a and b represent the spectra before and after a 1020 min UV irradiation, respectively. Referring to the literature on HI in the gas and in various rare gas matrixes,[12−14] which is schematically summarized in Figure 2, the spectrum in Figure 1a is divided into the three regions as shown by the horizontal arrows. In the region above ∼2210 cm^{-1}, two faint peaks are seen at 2229.1 and 2225.7 cm^{-1} which are associated with monomeric HI, whereas the rich absorptions at ∼2210 cm^{-1} to ∼2160 cm^{-1} are assigned to dimeric HI, and the very feeble absorptions below ∼2160 cm^{-1} amplified by a factor of 10 are attributed to trimeric HI. The infrared absorption of HI monomer in matrixes is known to be notoriously weak, and there is a statement in the literature that "the absorbance of monomer HI appears to be significantly weaker than the absorbance of HI that forms a hydrogen bond to another molecule. It is therefore difficult to observe monomer HI in a matrix without significant dimer absorption".[14] The faint and intense absorptions in the first two spectral regions in Figure 1a are consistent with the cited statement. The very weak absorption in the third region assigned to the trimeric system implies that the absolute

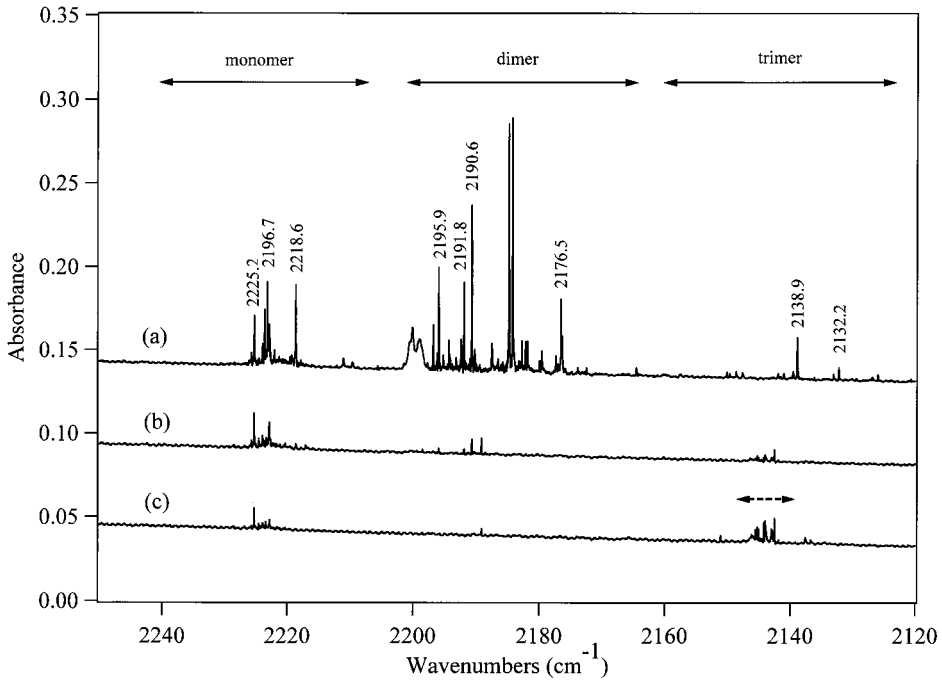

Figure 3. FTIR spectra in the HI stretching region of sample in solid parahydrogen with a composition of CO_2/HI/*p*-H_2 = 15:1:2×10^6: (a) the sample immediately after the deposition; (b) same as (a) after an initial 180 min UV irradiation; (c) same as (b) after an additional 240 min irradiation followed by a dark period of 300 min and a further irradiation for 240 min. Thus, the total irradiation time amounts to 180 + 240 × 2 = 660 min. The peaks shown with frequencies appear newly contrary to the case of Figure 1a. The dashed-line arrow in (c) shows the CO stretching vibration. The multiple peaks may reflect the subtle difference of the environment of CO.

concentration of the trimers is very small, which is reasonable if the dimerization is the dominant process in the impinging premixed gas before the crystallization in the optical cell (see the Experimental Section).

Since most of the HI molecules in the premixed gas have little chance to encounter CO_2 because of the low ratio of CO_2/HI = 1:16, most of the peaks are regarded as due to the monomers, dimers, and trimers of HI uncomplexed with CO_2. Since the two peaks at 2229.1 and 2225.7 cm^{-1} barely appear in the sample of a high ratio of CO_2/HI = 15:1, which is discussed in the next subsection, we attribute the two peaks to two different HI monomers uncomplexed with CO_2, although we have no definite interpretation of the appearance of the *two* peaks at the moment. In passing, we note that the structure reported for monomeric HI in Ar matrix[14] is absent in solid *p*-H_2. Furthermore, we note from Figure 2 that the frequencies of monomeric HI in *p*-H_2 are red-shifted by ∼10−20 cm^{-1} relative to those in Ar while those of dimeric and trimeric HI in *p*-H_2 are comparable to those in Ar.

As shown in Figure 1b almost all the peaks disappeared after a continual 1020 min irradiation. No significant new absorption appeared in the spectral region from 4000 to 1000 cm^{-1} except those at 7639.2, 7638.5, and 7637.8 cm^{-1}. These are assigned to the spin−orbit absorption of the iodine atom,[8] the details of which will be published in a separate paper.[9] Therefore, in the sample of CO_2/HI = 1:16 the major event of photolysis must be the photodissociation of the HI moiety.

3.2. System of CO_2/HI/*p*-H_2 = 15:1:2×10^6. The spectra of the sample with a composition of CO_2/HI/*p*-H_2 = 15:1:2×10^6 in the HI absorption region are shown in Figure 3. The composition was chosen to have CO_2 overwhelmingly relative to HI. Traces a−c represent spectra before UV irradiation (a), after a 180 min irradiation (b), and after an additional irradiation of 240 min plus a dark period of 300 min plus a further 240 min irradiation to make the total irradiation time equal to 660 min (c). Comparison of trace a of Figures 1 and 3 indicates that new absorptions appear in Figure 3 at around 2225−2220, 2195−2175, and 2150−2130 cm^{-1}, the wavenumbers of the major peaks being given in the figure. Since the difference between the two samples should be attributed to the difference of the relative concentration of CO_2 over HI, the much stronger absorptions under the arrow "monomer" are assigned to the monomeric HI affected by CO_2. Similarly, the newly appearing peaks under the arrows "dimer" and "trimer" are attributed to $(HI)_2$ and $(HI)_3$ moieties interacting with CO_2. Here, the notation of CO_2 does not necessarily mean a single CO_2 molecule but small clusters of $(CO_2)_n$ (n = 1, 2, ...), because a supplementary experiment of CO_2/*p*-H_2 systems under the same experimental condition indicates the formation of the clusters (see Figure 5 below).

Comparison of traces a and b in Figure 3 shows that after an initial 180 min irradiation the absorptions in the dimer and trimer regions vanish almost completely, whereas the decrease of the absorption in the monomer region is a little reluctant. The additional irradiation for 240 × 2 min further changes the spectrum from trace b to c in Figure 3. The decrease is accompanied with the appearance of new absorptions at around 2145−2140 cm^{-1}, as shown under the dashed-line arrow in Figure 3c. The new peaks are assigned to carbon monoxide in reference to a reported peak of CO in Ar matrix at 2148.8 cm^{-1}.[15] Recently, Fajardo et al. observed the absorption of CO in the similar spectral region by their rapid deposition technique.[16]

Panels a and b in Figure 4 demonstrate the temporal change of the integrated intensities of the absorption in the HI stretching region for HI···$(CO_2)_n$ and $(HI)_2$···$(CO_2)_n$, respectively, as a function of UV irradiation time and standing period under dark. Panel c shows the accompanying change of the intensity of the CO absorption. The increase in the CO absorption is correlated with the decrease in the absorption of HI···$(CO_2)_n$ in the first irradiation and reirradiation periods. However, the $(HI)_2$···$(CO_2)_n$ rapidly decreases to zero in the initial irradiation period, and

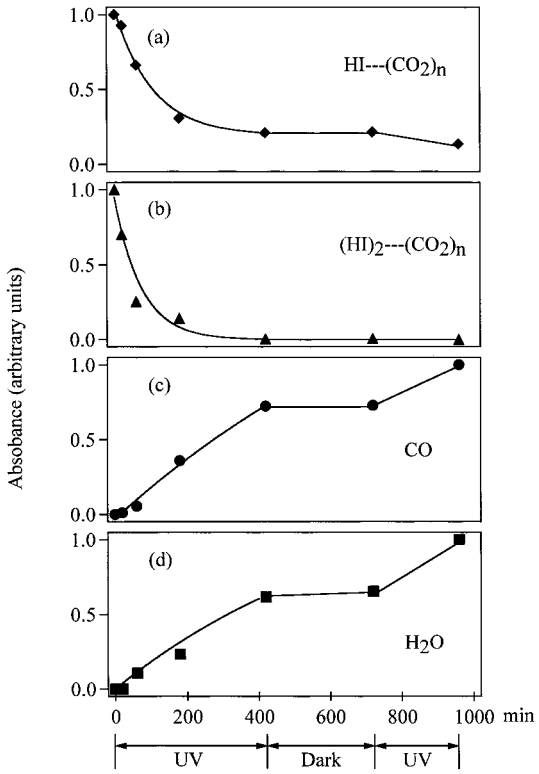

Figure 4. The upper two panels show the temporal change of the integrated intensities of the HI stretching vibration for monomeric HI and $(HI)_2$ complexed with small CO_2 clusters. The plots are obtained by the integration of peaks under the arrows of "monomer" and "dimer" spectral regions in Figure 3. The lower two panels are obtained by plotting the integrated intensity of the CO stretching vibration in Figure 3c and the intensity of the antisymmetric stretching vibration of H_2O shown in the right-hand-side of Figure 6, respectively. The horizontal portions in the eye-guide curves denoted by "Dark" corresponds to a 300 min dark period at 4.9 K. Except for this period, the abscissa is for the UV irradiation time.

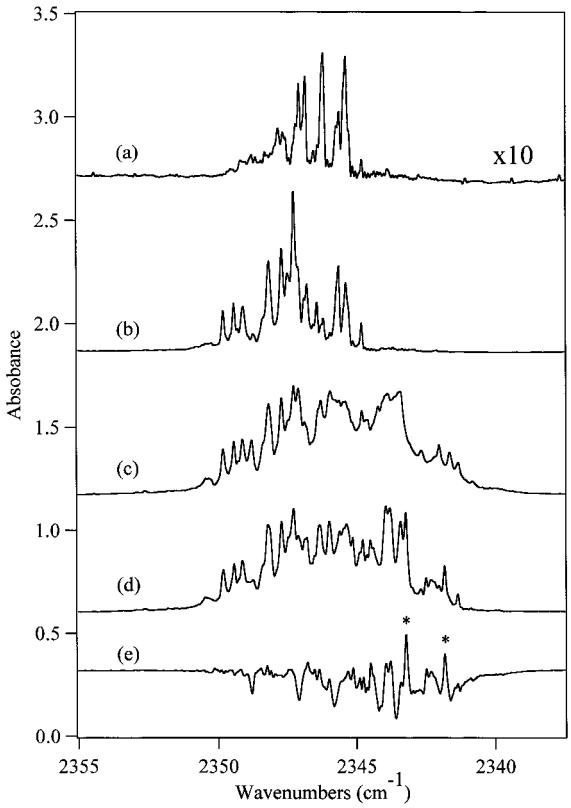

Figure 5. The upper two panels show the spectra in the antisymmetric stretching region of CO_2 for $CO_2/p\text{-}H_2$ samples. The ratio of CO_2 of (a) over (b) is about 1:400. Both spectra are unaffected by prolonged UV irradiations. The lower two panels are for the same sample as for Figure 3. Traces c and d correspond to traces a and c in Figure 3, respectively. Trace e is the difference between traces d and c. The downward dips and a few overshoots with the asterisks are explained in the text.

there is no correlation between $(HI)\cdots(CO_2)_n$ and CO. As for the last panel d in Figure 4 arguments will be postponed until the end of this section.

Traces a and b in Figure 5 demonstrate the absorption in the spectral region of the ν_3 antisymmetric stretching vibration of CO_2 for $CO_2/p\text{-}H_2$ systems without HI. The concentration ratio of CO_2 is 5a/5b $\cong$ 1:400. The difference of the spectra between the two systems indicates the formation of CO_2 clusters of different sizes. The dimer formation of CO_2 in Ar matrix is reported earlier.[17] Also, CO_2 clusters up to tetramers are reported for a three-component system of CO_2/HCl/Ar, which resembles the present system.[18] Both spectra in traces a and b in Figure 5 did not change upon irradiation with full UV light from the lamp for 300 min, and no appearance of CO was observed, in contrast to the case for Figure 3.

Trace c in Figure 5 demonstrates the ν_3 mode of CO_2 for the sample giving the spectrum of the HI stretching in Figure 3a. After a total of 660 min irradiation, the spectrum in trace c changed to trace d in Figure 5, in contrast to the photoinsensitive systems giving the spectra in traces a and b. The difference of between traces d and c is shown in trace e in Figure 5, which indicates that the downward dips predominate over the upward shoots at lower frequencies. In consistence with the downward dips, the integrated intensity of the spectrum in Figure 5d is about 20% less than that in Figure 5c. Such a decrease must be ascribed to CO_2 in $HI\cdots(CO_2)_n$ and $(HI)_2\cdots(CO_2)_n$ complexes because in the $CO_2/p\text{-}H_2$ system there is no such decrease in the CO_2 absorption.

A similar trend of the overall decrease is observed also in the ν_3 region of $^{13}CO_2$ which is present in the natural abundance in the sample, as shown in the left-hand-side panel of Figure 6. Traces a and b in the left-hand-side panel of Figure 6 are for the sample giving the spectra in traces a and b of Figure 3 as well as traces c and d of Figure 5. The difference between traces b and a is shown in trace c in the left-hand-side panel of Figure 6. As for a few upward shoots designated with the asterisks in both trace e in Figure 5 and trace c in the left-hand-side panel of Figure 6, an explanation will be given in the next section.

The right-hand-side panel of Figure 6 shows the FTIR spectrum of the rotationally resolved antisymmetric stretching vibration of H_2O. The peaks at 3765.7, 3763.6, and 3762.4 cm^{-1} in trace a of the right-hand-side panel of Figure 6 are due to the residual water vapor in the optical path. These unwanted peaks are absent in traces b and c in the right-hand-side panel of Figure 6 by fortuitous cancellation of the background signal of moisture. Instead, there appears a newly growing peak at 3765.5 cm^{-1} which is slightly red-shifted against the peak at 3765.7 cm^{-1} in trace a. This new peak is assigned to H_2O produced by UV irradiation *in* the solid $p\text{-}H_2$ in reference to the absorption at 3734.3 cm^{-1} in Ar matrix.[19] The peak begins to appear in the initial irradiation for 180 min and continues to grow in the subsequent irradiation for 240 min. It remains unchanged in the next dark period for 300 min until it restarts to grow in the reirradiation period for 240 min. The temporal behavior of this H_2O peak is shown in Figure 4d, which is in parallel with the behavior of the absorption of CO as shown in

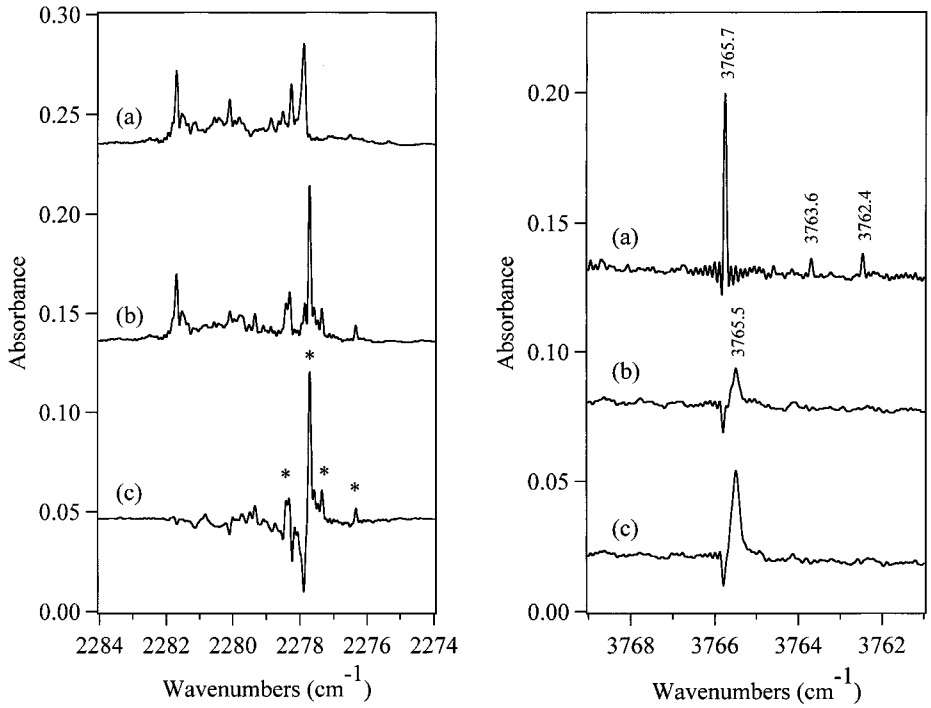

Figure 6. (left) Spectra in traces a and b represent the $^{13}CO_2$ antisymmetric stretching region for the sample giving the spectra in Figure 3. They correspond to the sample before and after irradiation, respectively, and trace c is the difference between traces b and a. The three correspond to spectra in traces c−e in Figure 5 for the $^{12}CO_2$ absorption. (right) A portion of the rotation−vibration spectrum of H_2O in the antisymmetric stretching region for the sample giving the spectra in Figure 3. Trace a is for the sample before UV irradiation. The three peaks at 3765.7, 3763.6, and 3762.4 cm^{-1} are the signals due to residual moisture in the optical path that failed to be canceled. Trace b is after 180 min UV irradiation, and trace c is after further irradiation for 480 min. The peak at 3765.5 cm^{-1}, slightly shifted from the peak at 3765.7 cm^{-1} for gaseous H_2O, is due to H_2O produced in solid *p*-H_2 by the reaction discussed in text.

Figure 4c. The parallel behavior of CO and H_2O definitely indicates that their production is synchronized.

4. Discussion

From Figures 3−6 it is seen that photolysis of the system of CO_2/HI/*p*-H_2 = 15:1:2×10^6 in section 3.2 induces the decrease in the absorptions of the spectral regions of both the HI stretching and the antisymmetric stretching vibration of CO_2 accompanied by the increase in the absorption of CO and H_2O. Thus, the generation of the CO and H_2O must be related to a photochemical decomposition of HI···$(CO_2)_n$ complexes. We propose the following reactions in the complexes:

$$HI + h\nu \rightarrow H^* + I \quad (1)$$

$$H^* + CO_2 \rightarrow HOCO^{\#} \rightarrow OH + CO \quad (2)$$

$$OH + H_2 \rightarrow H_2O + H \quad (3)$$

To rationalize the scheme, we have collected relevant energetic information from various sources in the literature[20−22] and collectively illustrated in Figure 7. Since the numerical values in the figure are for the gas-phase reactions or for those obtained by computation, the small stabilization energy from the formation of the van der Waals complexes in the present work in the *p*-H_2 matrix is not taken into account. The lower left-hand-side corner in the figure represents the initial state, while the right-most end corresponds to the final state. Since the dissociation energy of HI is 3.05 eV,[23] the excess energies upon the UV excitation at 253.7 nm (=4.88 eV) are 1.83 and 0.88 eV for the production of I($^2P_{3/2}$) and I($^2P_{1/2}$), respectively. The excess energy is mainly transferred to the translational energy of the split H atom because of the heavy mass of I atom. Since the broad ultraviolet absorption of HI is composed of three

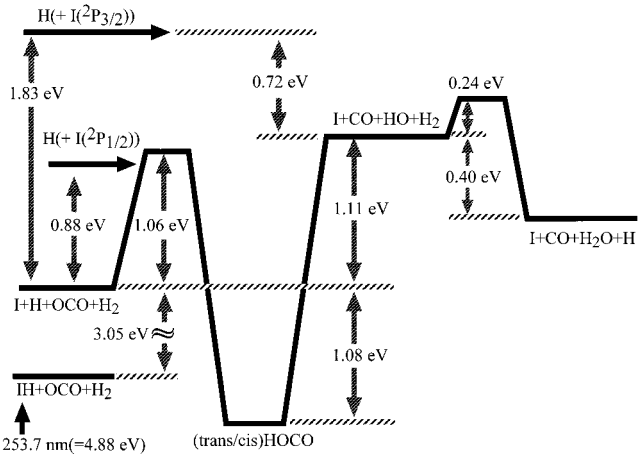

Figure 7. Energy diagram relevant to analyze the photochemical processes of HI···CO_2 complexes. Numerical values are collected from various sources in the literature.[20−22]

different excited states, the branching ratio of I($^2P_{3/2}$) and I($^2P_{1/2}$) is wavelength dependent. It is reported that at 266 nm excitation about 64% of the I atom is in the ground $^2P_{3/2}$ state[24] and that at a wavelength of 253.7 nm used in the present work the percentage of the excited iodine atoms is about 66%.[25] As shown in the left-hand side of Figure 7, the kinetic energy of 1.83 eV of the hydrogen atoms produced with I($^2P_{3/2}$) is sufficient to surmount the 1.06 eV activation barrier for the reaction between H and CO_2 with an approximately 0.8 eV surplus energy at the barrier top (see refs 22, 26, 27, and references therein). On the other hand, the H atom formed with I($^2P_{1/2}$) does not have enough energy to overcome the reaction barrier of 1.06 eV.

The reaction of H atoms with carbon dioxide is known to proceed via the intermediate HOCO.[28−30] The intermediate

species in solid Ar is characterized by Milligan and Jacox, the strongest absorptions being at 1843.6 and 1211.3 cm^{-1}.[31,32] The lifetime of the intermediate in the gas phase is reported to be a few picoseconds.[29,30] Consistently, the formation of the OH radical in the gas-phase photolysis of HI and CO_2 at about 253.7 nm is reported to occur on a subpicosecond time scale.[33]

These pieces of information lead immediately to reactions 1 and 2. As for reaction 3, the diagram in Figure 7 indicates that the excess energy of 0.72 eV may yield initially hot OH radicals which may react easily with the surrounding hydrogen molecules. Since the activation energy for this reaction is about 0.24 eV, one may expect the detection of the OH radical if it is relaxed quickly to the ground state. However, the absorption of the OH radical reported at 3554.1 cm^{-1} for an Ar matrix[34] was not detected in the present work, which implies either the radical is hot enough to surmount the barrier of 0.24 eV in Figure 7 or the relaxed radical may tunnel to the system in the time scale of the present experiment. The latter possibility is intriguing because it is proposed that tunneling reactions of neutral radicals with the hydrogen molecule may proceed fast if the reactions are exothermic enough.[35]

In any event, the indication of a rapid reaction of the OH radical with the hydrogen molecule ensures the correlation of the formation of CO and H_2O. According to the literature, excitation of the OH radical to either the first or the second excited vibrational state enhances the rate of reaction 3 only by less than 50%, while the excitation of the H_2 molecule to the $v = 1$ state increases the rate by a factor of 150.[36,37] How relevant this information to the present study in the solid hydrogen is yet to be pursued.

Weakly bound complexes in the gas phase often possess well-defined structures. For example, the HF and HCl complexes with the CO_2 molecule are linear[38] while the HBr complex has a slanted T-shape for the Br···CO_2 skeleton with the molecular axes being nearly perpendicular and the distance between the centers of mass of the two components being about 3.6 Å.[39] This structure has been confirmed in pulsed nozzle FT-MW measurements also.[40,41] However, there seems no structural study on the HI···CO_2 complex in the gas phase. Therefore, we have no definite idea on the structure of the assumed complexes between HI and CO_2 in the *p*-H_2 matrix. The appearance of a multitude of peaks even in HI···$(CO_2)_n$ system may suggest the coexistence of a number of local minima on the energy surface of the complexes, each minimum corresponding to a structure and to a particular spectral peak. The preferential disappearance of some peaks in the HI stretching region (Figure 3) as well as in the CO_2 ν_3 region (traces c vs d in Figure 5 and traces a vs b in the left-hand-side panel of Figure 6) may indicate that there is a distribution of the relative orientation and/or the distance between HI and the counterpart interacting $(CO_2)_n$ ($n = 1, 2,$ ...) and that in some complexes the coupled reactions 1 and 2 proceed preferentially. It is desirable to disclose the structure of each complex and correlate the structure with the chemical reactivity.

As shown in Figure 4, the rapid decrease of the $(HI)_2$···$(CO_2)_n$ in the initial stage of UV irradiation is not correlated with growth of CO and H_2O. Although not shown in the figure, the very weak $(HI)_3$···$(CO_2)_n$ signal in Figure 3a also behaved similarly to the $(HI)_2$···$(CO_2)_n$ complexes. The result is reasonable because the dominant photochemical process in the dimeric HI system is considered to be one-photonic, that is, $(HI)_2 + h\nu \rightarrow H_2 + I_2$ in view of our study of photolysis of $(CH_3I)_2$[42] and $(C_2H_5I)_2$[43] in solid *p*-H_2, where we observed an efficient production of C_2H_6 and disproportionation of the ethyl radical, respectively. Previously, Donaldson et al. also reported the reaction, $(HI)_2 + h\nu \rightarrow H_2 + I_2$, in the molecular beam.[44]

The possibility that CO and H_2O originate from the photolysis at 184.9 nm of CO_2 is ruled out because no spectral change occurred in the CO_2/*p*-H_2 systems as mentioned in connection with traces a and b in Figure 5. We examined the other possibility of the formation of H_2O via the photolysis at 184.9 nm of the OH radical in reaction 3 because the dissociation energy of the radical of 4.35 eV[45] is lower than the photon energy of 184.9 nm. However, this possibility is slim unless the OH radical absorbs the second photon with an extreme efficiency to yield the reactive O atom. The decrease of a part of the ν_3 absorption of CO_2 shown in trace e of Figure 5 and in trace c of the left-hand-side panel of Figure 6 along with the synchronous formation of CO and H_2O are now firmly attributed to the consecutive reactions 2 and 3 which are initiated by the absorption of light by the HI moiety in the HI···$(CO_2)_n$ complexes.

We now consider a few upward shoots in trace e of Figure 5 and trace c in the left-hand-side panel of Figure 6 designated with the asterisks. As mentioned in connection with Figure 7, the photolysis of HI at 253.7 nm is reported to yield a pair of $I(^2P_{3/2}) + H^*$ (~1.83 eV) and a pair of $I(^2P_{1/2}) + H^*$ (~0.88 eV) in an approximate ratio of 1:2. So far, we have focused on the processes initiated by the former only. As for the latter, to produce the less energetic H atoms, the consecutive reactions 2 and 3 are prohibitive so that the counterpart $I(^2P_{1/2})$ may quickly relax to $I(^2P_{3/2})$ and form a loose complex with $(CO_2)_n$. Such a complex between $(CO_2)_n$ and the very polarizable I atom is expected to give red-shifted $(CO_2)_n$ absorptions.

In conclusion, we have successfully observed the consecutive reactions of one of the CO_2 molecules in HI···$(CO_2)_n$ complexes with an H atom produced by the photolysis of HI to give the products OH + CO, which is followed by $OH + H_2 \rightarrow H_2O + H$. The salient feature of the present work is that we employed the van der Waals complex as the dopant in the *p*-H_2 matrix. Since the geometrical structure of the complex in the matrix is fixed, the system is reminiscent of the "precursor-geometry-limited" method in the gas-phase study which was introduced by Jouvet and Soep[46,47]and by the Wittig group,[48−50] and is extensively developed notably by Zewail[30] and Wittig.[20]

Lastly, we should like to point out that the present system is closely related to the intensively studied four-atom reactions of $OH + CO \rightarrow CO_2 + H$ and $OH + H_2 \rightarrow H_2O + H$. The former is regarded as an important reaction in combustion. The latter is responsible for the chain propagation in the hydrogen combustion. These reactions are the subject of the highly sophisticated theoretical study also. Comprehensive references are in the recently published papers.[22,26,27] We hope that the present approach provides complementary information to the gas-phase experimental as well as the theoretical studies.

Acknowledgment. The study was partially supported by a Grant-in-Aid for Scientific Research of the Ministry of Education, Science, Culture, and Sports of Japan. M. Räsänen acknowledges support from the Academy of Finland.

References and Notes

(1) See, for example: Brus, L. E.; Bondybey, V. E. *J. Chem. Phys.* **1976**, *65*, 71.
(2) Oka, T. *Annu. Rev. Phys. Chem.* **1993**, *44*, 299.
(3) Momose, T.; Shida, T. *Bull. Chem. Soc. Jpn.* **1998**, *71*, 1.
(4) Fajardo, M. E.; Tam, S.; Thompson, T. L.; Cordonnier, M. E. *Chem. Phys.* **1994**, *189*, 351.
(5) Momose, T.; Uchida, M.; Sogoshi, N.; Miki, M.; Masuda, S.; Shida, T. *Chem. Phys. Lett.* **1995**, *246*, 583.

(6) Fushitani, M.; Sogoshi, N.; Wakabayashi, T.; Momose, T.; Shida, T. *J. Chem. Phys.* **1998**, *109*, 6346.
(7) Momose, T.; Hoshina, H.; Sogoshi, N.; Katsuki, H.; Wakabayashi, T.; Shida, T. *J. Chem. Phys.* **1998**, *108*, 7334.
(8) Pettersson, M.; Nieminen, J. *Chem. Phys. Lett.* **1998**, *283*, 1.
(9) Fushitani, M.; Sogoshi, N.; Wakabayashi, T.; Momose, T.; Shida, T. Unpublished.
(10) Hoffman, C. J. *Inorg. Synth.* **1963**, *7*, 180.
(11) Tam, S.; Fajardo, M. E.; Katsuki, H.; Hoshina, H.; Wakabayashi, T.; Momose, T. *J. Chem. Phys.* **1999**, *111*, 4191.
(12) Kunttu, H. M.; Seetula, J. A. *Chem. Phys.* **1994**, *189*, 273.
(13) Bowers, M. T.; Flygare, W. H. *J. Chem. Phys.* **1966**, *44*, 1389.
(14) Engdahl, A.; Nelander, B. *J. Phys. Chem.* **1986**, *90*, 6118.
(15) Dubost, H.; Abouaf-Marguin, L. *Chem. Phys. Lett.* **1972**, *17*, 269.
(16) Fajardo, M. E.; Tam, S. 53rd Ohio State University International Symposium on Molecular Spectroscopy, FC05, Columbus, OH, 1998.
(17) Guasti, R.; Schettino, V.; Brigot, N. *Chem. Phys.* **1978**, *34*, 391.
(18) Fourati, N.; Silvi, B.; Perchard, J. P. *J. Chem. Phys.* **1984**, *81*, 4737.
(19) Ayers, G. P.; Pullin, A. D. E. *Spectrochim. Acta A* **1976**, *32*, 1629.
(20) Jaques, C.; Valachovic, L.; Ionov, S.; Bömer, E.; Wen, Y.; Segall, J.; Wittig, C. *J. Chem. Soc., Faraday Trans.* **1993**, *89*, 1419.
(21) Alagia, M.; Balucani, N.; Casavecchia, P.; Stranges, D.; Volpi, G. G. *J. Chem. Phys.* **1993**, *98*, 8341.
(22) Loomis, R. A.; Lester, M. I. *Annu. Rev. Phys. Chem.* **1997**, *48*, 643.
(23) Huber, K. P.; Herzberg, G. *Molecular Spectra and Molecular Structure. IV. Constants of Diatomic Molecules*; Van Nostrand: New York, 1979.
(24) Clear, R. D.; Riley, S. J.; Wilson, K. R. *J. Chem. Phys.* **1975**, *63*, 1340.
(25) Langford, S. R.; Regan, P. M.; Orr-Ewing, A. J.; Ashfold, M. N. R. *Chem. Phys.* **1998**, *231*, 245.
(26) Clary, D. C. *J. Phys. Chem.* **1994**, *98*, 10678.
(27) Alagia, M.; Balucani, N.; Casavecchia, P.; Stranges, D.; Volpi, G. G. *J. Chem. Soc., Faraday Trans.* **1995**, *91*, 575.
(28) Chen, Y.; Hoffmann, G.; Oh, D.; Wittig, C. *Chem. Phys. Lett.* **1989**, *159*, 426.
(29) Scherer, N. F.; Khundkar, L. R.; Bernstein, R. B.; Zewail, A. H. *J. Chem. Phys.* **1987**, *87*, 1451.
(30) Scherer, N. F.; Sipes, C.; Bernstein, R. B.; Zewail, A. H. *J. Chem. Phys.* **1990**, *92*, 5239.
(31) Milligan, D. E.; Jacox, M. E. *J. Chem. Phys.* **1971**, *54*, 927.
(32) Jacox, M. E. *J. Chem. Phys.* **1988**, *88*, 4598.
(33) Ionov, S. I.; Brucker, G. A.; Jaques, C.; Valachovic, L.; Wittig, C. *J. Chem. Phys.* **1992**, *97*, 9486.
(34) Pehkonen, S.; Pettersson, M.; Lundell, J.; Khriachtchev, L.; Räsänen, M. *J. Phys. Chem. A* **1998**, *102*, 7643.
(35) Herbst, E. *Annu. Rev. Phys. Chem.* **1995**, *46*, 27.
(36) Zellner, R.; Steinert, W. *Chem. Phys. Lett.* **1981**, *81*, 568.
(37) Glass, G. P.; Chaturvedi, B. K. *J. Chem. Phys.* **1981**, *75*, 2749.
(38) Baiocchi, F. A.; Dixon, T. A.; Joyner, C. H.; Klemperer, W. *J. Chem. Phys.* **1981**, *74*, 6544.
(39) Zeng, Y. P.; Sharpe, S. W.; Shin, S. K.; Wittig, C.; Beaudet, R. A. *J. Chem. Phys.* **1992**, *97*, 5392.
(40) Rice, J. K.; Lovas, F. J.; Fraser, G. T.; Suenram, R. D. *J. Chem. Phys.* **1995**, *103*, 1263.
(41) Sharpe, S. W.; Zeng, Y. P.; Wittig, C.; Beaudet, R. A. *J. Chem. Phys.* **1990**, *92*, 943.
(42) Momose, T.; Miki, M.; Uchida, M.; Shimizu, T.; Yoshizawa, I.; Shida, T. *J. Chem. Phys.* **1995**, *103*, 1400.
(43) Sogoshi, N.; Wakabayashi, T.; Momose, T.; Shida, T. *J. Phys. Chem. A* **1997**, *101*, 522.
(44) Fan, Y. B.; Randall, K. L.; Donaldson, D. J. *J. Chem. Phys.* **1993**, *98*, 4700.
(45) Herzberg, G. *Molecular Spectra and Molecular Structure. I. Spectra of Diatomic Molecules*, 2nd ed.; Van Nostrand: New York, 1950.
(46) Jouvet, C.; Soep, B. *Chem. Phys. Lett.* **1983**, *96*, 426.
(47) Jouvet, C.; Soep, B. *J. Chem. Phys.* **1984**, *80*, 2229.
(48) Buelow, S.; Radhakrishnan, G.; Catanzarite, J.; Wittig, C. *J. Chem. Phys.* **1985**, *83*, 444.
(49) Radhakrishnan, G.; Buelow, S.; Wittig, C. *J. Chem. Phys.* **1986**, *84*, 727.
(50) Buelow, S.; Noble, M.; Radhakrishnan, G.; Reiseler, H.; Wittig, C.; Hancock, G. *J. Phys. Chem.* **1986**, *90*, 1015.